

A MEMS Tunable Inductor

I. Zine-El-Abidine*, M. Okoniewski* and J. G. McRory*

*University of Calgary and TRILabs
280, 3553 – 31 Street N.W. Calgary, AB, Canada
imed@cal.trilabs.ca

ABSTRACT

This paper reports a single-wafer micromachined radio-frequency (RF) inductor that can be integrated in a conventional RFIC device. The inductor achieved a quality factor greater than 9 at 5GHz and a self-resonance frequency well above 15 GHz. The inductor is tunable and the inductance variation is greater than 8%.

Keywords: Radio frequency, MEMS, inductor, tunable.

1 INTRODUCTION

RF inductors are needed in any wireless front-end circuitry; the performance of both transceivers and receivers depends heavily on this component. High-Q inductors reduce the phase noise and the power consumption of VCO's and amplifiers and reduce the return loss of matching networks and filters. The quality factor of inductors can be increased by using a thick metal layer [1], [5] and by isolating the inductor from the substrate [2]-[6]. To isolate the inductor, bulk micromachining [2]-[5] or self-assembly [7], [8] can be used. Further, tunable inductors allow for performance optimization of RF front-end circuits. To date, there has not been a practical implementation of a high-Q tunable inductor. Most of the reported MEMS inductors are static fixed-value inductors. One variable inductor using MEMS switches has been reported [9]. However, it provides only discrete values of inductance depending on the ON/OFF configuration of the switches. A tunable inductor using self-assembly technique [8] has been reported. The drawback of that device is that such inductor, are lifted from the substrate, thus becoming prone to electromagnetic interference in the transceiver system.

2 DESIGN

The inductor reported here is formed of two layers, the bottom layer is silicon nitride and the top layer is gold. To increase the quality factor at the high frequencies, the silicon underneath the inductor is etched away. To achieve the tunability, two inductors are connected in parallel. The

outer loop inductor is held to the substrate with nitride beams while the inner loop inductor is left free as shown in Figure 1.

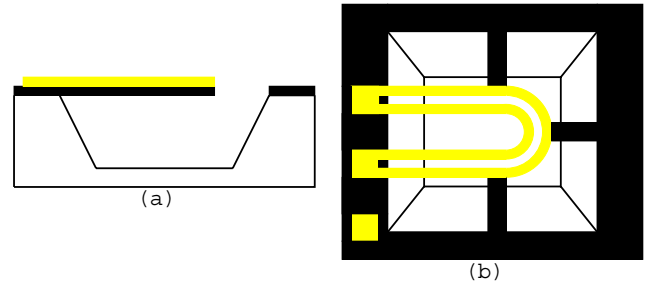


Figure 1: (a) side view, (b) top view of the inductor.

Since the inductors are made of two layers of different thermal expansion coefficients, they form a thermal bimorph [9], [10]. When a current is drawn through the inductors, it causes the inner inductor to move downwards into the pyramidal pit, while the nitride beams prevent the outer inductor from moving. The change of the angle between the two inductors results in a change in the mutual inductance and therefore the overall inductance.

3 FABRICATION

The fabrication process of the tunable inductor is shown in Figure 2. The process starts with depositing of a 600 nm nitride layer on the surface of the silicon wafer. The nitride layer is then etched using RIE (Reactive Ion Etching) to form the bottom layer of the inductor, the beams holding the outer loop and the cavity edges. Then, a 100 nm layer of chrome is deposited to serve as an adhesion layer for gold. The gold layer is 1 μ m thick. Gold and chrome are etched using iodine and nitric acid respectively. The final step is the bulk anisotropic etching using KOH to release the inductors and form the pyramidal pit. The silicon nitride layer played the role of the mask during the anisotropic etch step. The cavity depth is 300 μ m. A scanning electron microscopy (SEM) photograph of the tunable inductor structure is shown in Figure 3.

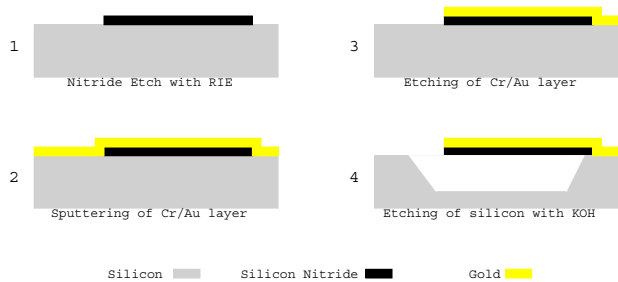


Figure 2: The fabrication process.

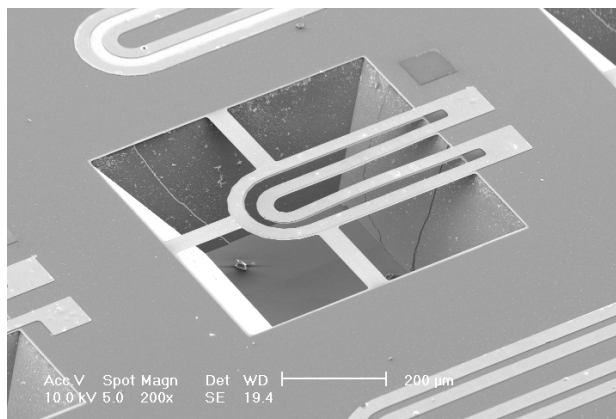


Figure 3: A SEM photograph of the inductor.

4 SIMULATION RESULTS

Figure 4 shows the simulated displacement versus the temperature difference using Coventorware [11]. The module used is MemETherm. Figure 5 shows the shape of the curved inner inductor.

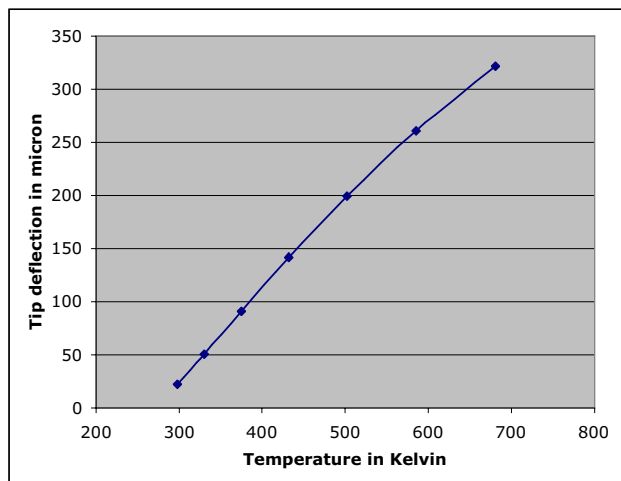


Figure 4: Simulated tip deflection versus temperature.

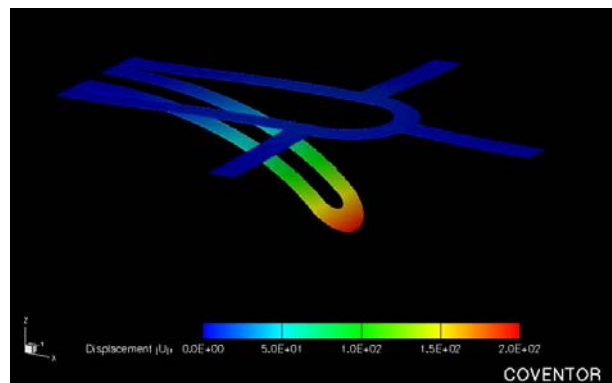


Figure 5: The simulated deflection of the inner inductor.

5 MEASURED RESULTS

The inductor was measured using 100- μm pitch ground-signal-ground (GSG) microwave probes connected to an HP8510 network analyzer with frequencies ranging from 1 GHz to 15 GHz. Probe calibration was done using Cascade CS-5 calibration substrate. Figure 6 illustrates the quality factor of the tunable inductor.

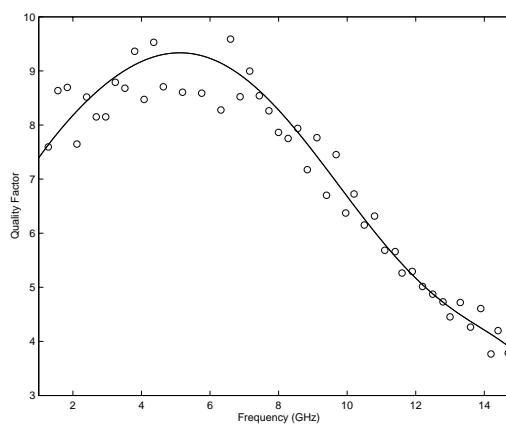


Figure 6: The quality factor of the inductor.

Figure 7 shows the tuning range of the inductor. The maximum value corresponds to the original state where the two inductors are at the same level. When the current flows through the two loops, the inner inductor deflects down as illustrated in Figure 8. By increasing the angle between the two loops, the mutual inductance decreases and therefore the overall inductance. The tuning range is 8%.

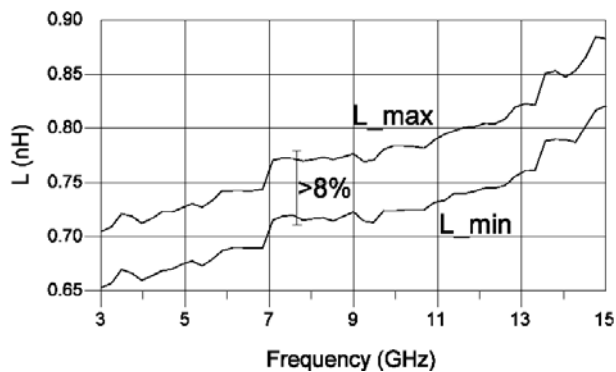


Figure 7: The inductance variation.

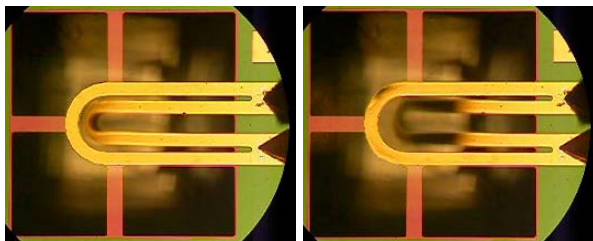


Figure 8: The deflection of the inner inductor under DC current.

6 CONCLUSION

A tunable MEMS inductor has been demonstrated with a tuning range of 8%. The inductor can operate beyond 15 GHz. The tunability is achieved using the principle of the bimorph actuation. Further improvements are underway to increase the quality factor and the tuning range.

7 ACKNOWLEDGMENT

The authors wish to thank Dr. Ken Westra, Stephanie Bozic, Dione Chambers and Hue Nguyen from the Nanofab of the University of Alberta for their assistance during the fabrication and Richard Humphrey from the Microscopy and Imaging Facility for his assistance with the SEM photographs caption. The authors wish to thank also NSERC for their support.

REFERENCES

- [1] S. Pinel, F. Cros, S. Nuttinck, S-W. Yoon, M.G. Allen, and J. Laskar, "Very high-Q inductors using RF-MEMS technology for System-On-Package wireless communication integrated module," *IEEE MTT-S Digest*, 2003, pp. 1497-1500.
- [2] J. Y.-C. Chang, A. A. Abidi, and M. Gaitan, "Large Suspended Inductors and Their Use in a 2- μ m CMOS RF

Amplifier," *IEEE Electron Device Lett.*, Vol. 14, May 1993, pp. 246-248.

[3] H. Lakdawala, X. Zhu, H. Luo, S. Santhanam, L. R. Carley, and G. K. Fedder, "Micromachined High-Q Inductors in a 0.18- μ m Copper Interconnect Low-K Dielectric CMOS Process," *IEEE J. Solid-State Circuits*, Vol. 37, No. 3, March 2002, pp. 394-403.

[4] H. Jiang, Y. Wang, J-L. A. Yeh, and N. C. Tien, "On-Chip Spiral Inductors Suspended over Deep Copper-Lined Cavities," *IEEE Trans. Microwave Theory and Techniques*, Vol. 48, No. 12, Dec 2000, pp. 2415-2422.

[5] R. P. Ribas, J. Lescot, J-L. Leclercq, J. M. Karam, and F. Ndagijimana, "Micromachined Microwave planar Spiral Inductors and Transformers," *IEEE Trans. Microwave Theory and Techniques*, Vol. 48, No. 8, pp. 1326-1335, August 2000, pp. 1326-1335.

[6] J-B. Yoon, B-I. Kim, Y-S. Choi, and E. Yoon, "3-D Construction of Monolithic Passive Components for RF and Microwave ICs Using Thick-Metal Surface Micromachining Technology," *IEEE Trans. Microwave Theory and Techniques*, Vol. 51, No. 1, January 2003, pp. 279-288.

[7] G. W. Dahlmann, E. M. Yeatman, P. R. Young, I. D. Robertson, and S. Lucyszyn, "MEMS High Q Microwave Inductors Using Solder Surface Tension Self-Assembly," *IEEE MTT-S International Microwave Symposium Digest*, June 2001, pp. 394-403.

[8] V. M. Lubecke, B. Barber, E. Chan, D. Lopez, M. E. Gross, and P. Gammel, "Self-Assembling MEMS Variable and Fixed RF Inductors," *IEEE Trans. Microwave Theory and Techniques*, Vol. 49, No. 11, November 2001, pp. 2093-2098.

[9] W-H. Chu, M. Mehregany, and R. L. Mullen, "Analysis of Tip Deflection and Force of a Bimetallic Cantilever Microactuator," *J. Micromech. Microeng.*, Vol. 3, 1993, pp. 4-7.

[10] W. Peng, Z. Xiao, and K. R. Farmer, "Optimization of Thermally Actuated Bimorph Cantilevers for Maximum Deflection," *Nanotech Proceedings*, Vol. 1, pp. 376-379, 2003.

[11] MEMCAD User's Manual. Coventor, Inc., Cary, NC. [Online]. Available: <http://www.coventor.com>.